Spectral Minimum and Giant Enhancement in Photoelectron Spectra from Xenon Atoms Driven by Intense Midinfrared Laser Fields

Jingtao Zhang*

State Key Laboratory for High-Field Laser Physics, Shanghai Institute of Optical and Fine Mechanics, Chinese Academy of Sciences, Shanghai 201800, China

D.-S. Guo†

State Key Laboratory of Precision Spectroscopy, East China Normal University, Shanghai 200062, China and Department of Physics, Southern University and A&M College, Baton Rouge, Louisiana 70813, USA

(Received 19 June 2012; published 5 February 2013)

Our theoretical study shows that the spectral minimum and the giant enhancement structures observed in the high harmonic spectra also exist in the photoelectron spectra from driven Xe atoms. They are attributed to the inherent property of the radial part of the wave function of the Xe $5p$ subshell in momentum space. The spectral minimum is caused by the nodal point in the modulus of the radial wave function in momentum space, and the giant enhancement reflects the increase in magnitude of the modulus of the wave function. To observe these structures, midinfrared lasers of about 0.2 PW/cm^2 intensity are preferred. Employing circularly polarized laser light is suggested for exhibiting these structures in photoelectron spectra.

DOI: 10.1103/PhysRevLett.110.063002 PACS numbers: 32.80.Rm, 32.80.Fb, 42.65.Ky

When atoms and molecules are irradiated by intense laser light, harmonics with frequencies as high as several hundred times the fundamental one are generated. Harmonic spectra are characterized by a plateau following the fast decrease in the low-energy region and followed by a sharp cutoff [1]. However, recent studies disclosed a spectral minimum in the plateau region originating from the atomic and molecular structures [2–6]. Consequently, it appears necessary to seek the physical origin of the spectral minimum and to obtain new insights into the electronic dynamics in the attosecond time scale [7]. An understanding of the role of the atomic and molecular structures in harmonic spectra and above-threshold photoelectron spectra is expected to help in the tomographic reconstruction of the atomic and molecular states [8,9].

Recently, Shiner *et al.* reported a giant resonance structure in the harmonic spectrum generated from Xe atoms driven by midinfrared laser pulses [10]. The giant resonance structure denotes a sudden increase in the yields of harmonics around 100 eV. A minimum appears in the plateau region preceding this structure. The giant resonance structure is interpreted by these authors [10] as a consequence of the collective resonance of $4d$ electrons following an inner-shell transient energy exchange between the $4d$ and the $5p$ electrons of Xe atoms. Such a process seems to allow one to observe the inner-shell multielectron dynamics in the attosecond time scale. However, it is not clear as to how the returning $5p$ electron can exchange energy with an existing $4d$ electron in a full shell. The evidence to support this multielectron interpretation would seem inconclusive.

In this Letter, we apply a nonperturbative QED theory [11] to treat the high harmonic generation (HHG) [12] from Xe atoms driven by midinfrared laser pulses and to recover the minimum structure in the HHG spectra. Our calculation shows that the location of the spectral minimum is independent of the laser field. Harmonics between the minimum and the cutoff form an islandlike structure in the spectra. The islandlike structure exhibits a broad peak around 100 eV. What is the cause of the minimum in the HHG spectra? Does the islandlike structure form the giant resonance structure observed by Shiner *et al.*? In this Letter, we answer these questions with a quite different physical interpretation to the giant resonance structure. Our study shows that the modulus of a single-electron momentum wave function that is thoroughly light free can account for both the structure minimum and the islandlike structure.

Cross-checks in different, but related, physical processes are necessary to identify which interpretation reveals the true physics. An important candidate for these physical processes is the above-threshold ionization (ATI) accompanied by HHG [13]. Many features of ATI spectra are shared by the harmonic spectra. In the linear polarization case, both the ATI and the harmonic spectra exhibit a plateau following a fast decrease in the low-energy region that is in turn followed by a sharp cutoff in the high-energy region, exhibiting some similarity between ATI and HHG. Moreover, both the HHG and the ATI spectra satisfy the same scaling law [14–16]. We expect that the spectral minimum and the following enhancement observed in the harmonic spectra may also appear in the ATI spectra.

This Letter serves two purposes. One is to seek the physical origin of the spectral minimum structure and of the enhancement structure in the HHG spectra. The other is

to exhibit a counterpart of these structures in the ATI spectra. We calculate both the HHG spectra and the ATI spectra from driven Xe atoms. We show below that the spectral minimum structure and the enhancement one exist in both the HHG and the ATI spectra. Based on the input information in our calculation, we attribute these structures to the single-electron radial wave function of Xe $5p$ in momentum space, which is laser-field-free. In HHG, they are common for midinfrared lasers at an intensity of about 0.2 PW/cm^2 (1 PW $= 10^{15}$ W). In ATI, they are smeared by rescattered photoelectrons but still kept in the directly emitted photoelectrons. To illustrate these structures, we deliberately choose the laser light parameters so that the directly emitted photoelectrons stick out on the ATI spectra. The circularly polarized laser light is preferred for observing these structures.

In the nonperturbative QED treatment, the intermediate states of the photon-electron system are the quantum-field Volkov states [17]. The harmonics are generated during the transitions from a Volkov state to an atomic bound state following the excitation from the initial bound state to the Volkov state. The transition matrix element of the qth-order harmonic is given by [12]

$$T_{fi}^{q} = \Phi_f(\mathbf{P}_q) \sum_{j_i=j_0}^{\infty} (u_p - j_i)(j_i - u_p - e_b)^{1/2} \Phi_i(\mathbf{P}_{j_i}) \times \int d\Omega [\boldsymbol{\epsilon}'^{*} \cdot \boldsymbol{\epsilon} \mathcal{X}^{*}_{-j_i}(z, \eta) \mathcal{X}_{-j_f-1}(z, \eta) + \boldsymbol{\epsilon}'^{*} \cdot \boldsymbol{\epsilon}^{*} \mathcal{X}^{*}_{-j_i}(z, \eta) \mathcal{X}_{1-j_f}(z, \eta) + \text{c.c.}], \quad (1)$$

where Ω is the solid angle of $\mathbf{P}_j$, $E_b = e_b\omega$ is the binding energy, and $U_p = u_p\omega$ is the ponderomotive energy; $\boldsymbol{\epsilon}$ and $\boldsymbol{\epsilon}'$ denote the polarization vector of the laser field and the harmonics, respectively. The sum over j_i is performed from $j_0 = \text{int}[u_p + e_b] + 1$ to infinity and $j_f = j_i - q$. The generalized phased Bessel function $\mathcal{X}_j(z, \eta)$ is defined in Ref. [18]. The complex variables are defined as $z = 2\sqrt{u_p/m_e\omega}\mathbf{P} \cdot \boldsymbol{\epsilon}$ and $\eta = u_p/2$, respectively. The momenta $|\mathbf{P}_j| = \sqrt{2m_e\omega(j - u_p - e_b)}$ and $|\mathbf{P}_q| = \sqrt{2m_e\omega(q - e_b)}$ are obtained from energy conservation. In Eq. (1), the quantities $\Phi_i(\mathbf{P})$ and $\Phi_f(\mathbf{P})$ are the momentum wave functions of the initial and final states, respectively. After averaging over the magnetic quantum number, they reduce to the radial wave function in momentum space as [19]

$$\Phi_{\text{nl}}(|\mathbf{P}|) = \int_0^{\infty} r dr R_{\text{nl}}(r) j_l(|\mathbf{P}|r), \quad (2)$$

where n and l are, respectively, the principal and the orbital angular quantum numbers; $j_l(x)$ is the spherical Bessel function; and $R_{nl}(r)$ is obtained numerically from the Dirac-Hartree-Fock calculation.

Figure 1(a) depicts the calculated HHG spectrum for Xe atoms driven by a laser field of wavelength 1.8 μm and intensity 0.19 PW/cm^2. A striking feature is the deep minimum located at 74 eV in the plateau. This feature agrees well with the recent observation of Shiner *et al.* [10]. To recognize the physical origin of the spectral minimum, we calculate the HHG spectrum from an H $1s$ state driven by a laser field of wavelength 1.6 μm and intensity 0.27 PW/cm^2. In such a case, the dimensionless dynamic parameters $\{u_p, e_b, q\}$ are kept the same so that the dynamic response to their respective driven laser fields of the Xe $5p$ electron and the H $1s$ electron are equivalent [16]. This technique makes it possible to identify the origins of these structures. The spectral minimum is not found in the H $1s$ spectrum, as shown in Fig. 1(a). This excludes the possibility that the spectral minimum is purely due to the laser field and further indicates that this structure may stem from the property of the light-free Xe $5p$ state. To see how the ground-state electron affects the HHG spectra, we plot in Fig. 1(b) the square modulus of the momentum radial wave function $|\Phi_f(|\mathbf{P}|)|^2$. The H $1s$ wave function decreases monotonically with energy, while the Xe $5p$ wave function shows a nodal point at 62 eV. The minimum in the Xe $5p$ HHG spectrum corresponds to the nodal point in the Xe $5p$ momentum radial wave function. Their locations differ from each other by about 12.1 eV,

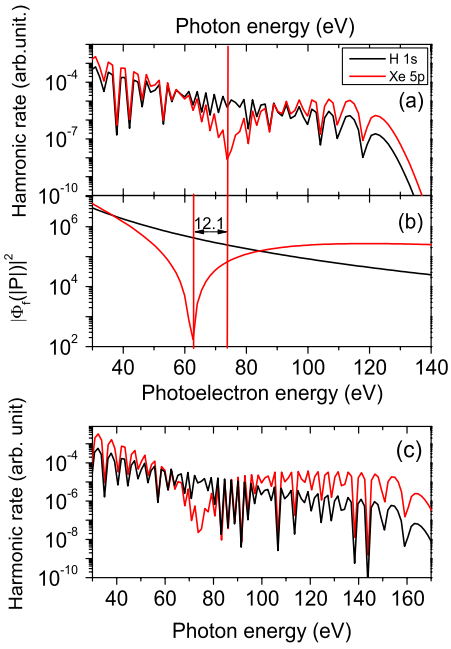

FIG. 1 (color online). (a) HHG spectra for the Xe $5p$ state and H $1s$ state. The laser fields are of wavelength 1.8 μm and intensity 0.19 PW/cm^2 for Xe and of wavelength 1.6 μm and 0.27 PW/cm^2 for H, respectively. (b) The square modulus of the wave function as a function of energy for H $1s$ state and for Xe $5p$ state, respectively. (c) Same as (a), but the laser intensity 0.25 PW/cm^2 for Xe and 0.36 PW/cm^2 for H, respectively. In (a) and (c), Xe $5p$ and H $1s$ denote the spectra for different wave functions. For clarity, the energy of H harmonics is divided by 1.12.

which coincides with the binding energy of Xe $5p$ electrons.

The harmonics between the minimum and the cutoff of the plateau form an islandlike structure and exhibit a broad peak around 100 eV. This structure looks similar to the giant resonance structure in Ref. [10]. In our treatment, this structure just manifests the increasing feature of the modulus square of the momentum radial wave function. It is determined by the property of the single-electron, light-free wave function. We term this structure as the giant enhancement. The starting point of the giant enhancement structure is independent of the laser field, but its ending point is subject to the cutoff energy, which depends on the laser field. Subsequently, the enhancement on the harmonic spectra becomes more evident as the laser-field intensity increases, as shown in Fig. 1(c).

A cross-check can be made with the comparison between the ATI spectra and their accompanying HHG spectra. However, 30 years after the observation of ATI [20], resonances reported in ATI spectra are all in outer-shell transitions, such as Freeman resonances [21–23]. The spectral minimum and the giant enhancement originating from a single atomic state are never reported. We now focus on how to illustrate these structures on the ATI spectra. The ATI electron rate is made by photoelectrons from two channels. One is for the directly emitted photoelectrons [15,24]

$$T_{fi}^{d} = (u_p - j_i)\mathcal{X}_{-j_i}(\zeta_f, \eta)^* \mathcal{X}_{-j_f}(\zeta_f, \eta)\Phi_i(|\mathbf{P}_f|), \quad (3)$$

in which j_i and j_f are the numbers of absorbed photons in the excitation and exit processes, respectively; the other is for the rescattered electrons

$$T_{fi}^{r} = \frac{im_e}{4\pi^{5/2}} \sum_{j_i} \mathcal{X}_{-j_f}(\zeta_f, \eta)(u_p - j_i)|\mathbf{P}_{j_i}|\Phi_i(|\mathbf{P}_{j_i}|) \times \int d\Omega_{\mathbf{P}} X_{q-j_i+j_f}(\zeta - \zeta_f)\mathcal{X}_{-j_i}(\zeta, \eta)^* \times U(\mathbf{P}_f - \mathbf{P} - q\mathbf{k}), \quad (4)$$

where $U(\mathbf{P})$ is the Fourier transform of the atomic binding potential and q denotes the ATI order. The calculated spectra for linear polarization exhibit the plateau structure with the cutoff at energy about $10U_p$, but those for circular polarization do not show any plateau.

The momentum radial wave function appears in the transition matrix elements of both the directly emitted and the rescattered photoelectrons. This means that the photoelectrons from the two channels carry the single-electron orbital information of the target atoms. For the directly emitted photoelectrons, although their angular distribution shows no dependence on the initial wave function [25], their yields are affected by the radial momentum wave function. As a result, the energy spectra of directly emitted photoelectrons should show the dependence on the initial electron state. For the rescattered photoelectrons, however, the correspondence between the yields and the momentum wave function becomes more complicated. Although the initial wave function appears in the rescattering amplitude T_{fi}^{r}, the amplitude varies with the momentum of photoelectrons in the Volkov states and also with the number of photons absorbed during excitation, say, j_i in Eq. (4). Because T_{fi}^{r} is a coherent sum over j_i, the interference effect smears out the information of a single-electron momentum wave function. To limit the loss of information on the initial wave function, one may select a case where the influence of rescattering photoelectrons is suppressed. For a linearly polarized laser, the plateau generally starts from $2U_p$. Below this limit, the directly emitted photoelectrons dominate the spectrum. This condition indicates that the usage of laser light with large U_p is beneficial. To obtain a larger U_p, one can increase the laser intensity or increase the laser wavelength, or do both. However, a more favorable choice is to use the circularly polarized laser so that the rescattering effect becomes negligible; thus, the directly emitted photoelectrons dominate the whole spectrum. Another advantage of using the circularly polarized laser is that the yield of the low-energy photoelectron is suppressed, so the structures in the higher-energy region become distinctive. We then show the spectral minimum and the giant enhancement in the ATI spectra produced by linearly and circularly polarized lasers, respectively.

We first calculate the ATI spectra in the linear polarization case. The featured location $2U_p$ on the ATI spectrum requires the least intensity of the driving laser light with a certain wavelength. The nodal point of the modulus of the Xe $5p$ momentum wave function appears at about 62 eV, which should be observed if the laser light satisfies the condition $U_p > 31$ eV so that 62 eV $< 2U_p$. For clarity, we also show the ATI spectra from the H $1s$ state for comparison.

Figure 2 depicts the ATI spectra at different wavelengths. There are three features to be noticed. The first one is that the minimum, located fixedly at 62 eV, appears only in Xe $5p$ ATI spectra. This feature indicates that the minimum originates from the light-free Xe $5p$ state. The correspondence in the ATI case is similar to that in the HHG case shown in Fig. 1(b) but without the binding energy shift. The second one is that the Xe $5p$ spectrum exceeds the H $1s$ spectrum from 85 eV; correspondingly, the Xe $5p$ wave function exceeds the H $1s$ wave function in magnitude. In the domain after the exceeding point, the Xe $5p$ ATI spectra are enhanced and the giant enhancement appears. The giant enhancement differs from any true resonant transition between atomic states, as it only relates to a single-electron atomic wave function that is light free and has nothing to do with transitions between two different atomic states. For example, the giant resonances in one-photon spectra were discussed extensively [26]; the

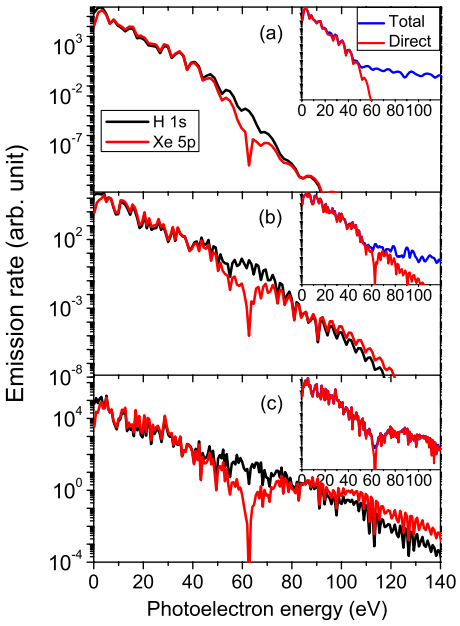

FIG. 2 (color online). Photoelectron spectra by linear polarization of wavelength (a) 0.8, (b) 1.3, and (c) 1.8 μm, respectively, and intensity 0.2 PW/cm^2. The main plots show the spectra for directly emitted photoelectrons. The insets show the Xe $5p$ spectra with and without the rescattered photoelectrons in blue and red, respectively.

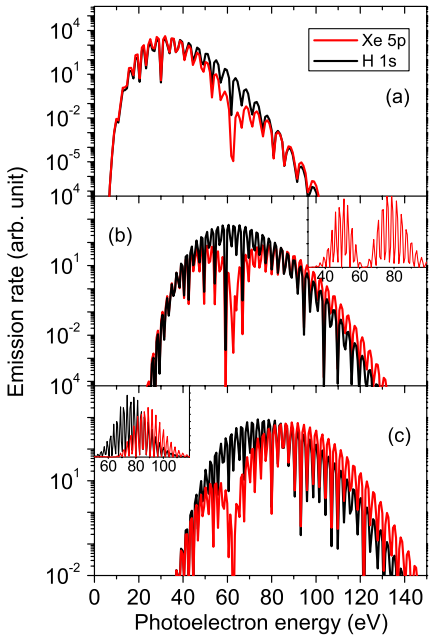

FIG. 3 (color online). Photoelectron spectra by circular polarization: (a) wavelength $\lambda = 1.3$ μm and intensity $I = 0.2$ PW/cm^2, (b) $\lambda = 1.8$ μm and $I = 0.18$ PW/cm^2, and (c) $\lambda = 1.8$ μm and $I = 0.25$ PW/cm^2. The insets depict the spectra in a linear scale.

giant enhancement in the current discussion involves as many as hundreds of photons in the infrared region. The third one is that the rescattered photoelectrons form a plateau that does not contain any minimum or enhancement, as is shown in the inset of Fig. 2(a). Consequently, the spectral minimum and the giant enhancement are cloaked by the rescattered photoelectrons in most cases. It is only in Fig. 2(c) that the spectral minimum and the giant enhancement become evident, where the rescattering effect is not overwhelming.

The above discussions indicate that, in the linear polarization case, the spectral minimum and the giant enhancement can be observed with special cares in choosing the laser parameters including the high intensity as a prerequisite condition. The main difficulty in this case is the low yields of these high-energy photoelectrons. The photoelectron rates at the giant enhancement region are, generally, at least 5 orders of magnitude lower than the highest rate. Moreover, in practice, the rescattered photoelectrons released at lower intensities obscure the spectral minimum. Thus, we turn our attention to the ATI spectra in the circular polarization case. Figure 3 depicts the ATI spectra from the Xe $5p$ state and the H $1s$ state driven by laser light of different intensities and some different wavelengths. The subplot (a) is for the laser of wavelength 1.3 μm and intensity 0.2 PW/cm^2 in which the spectral minimum is evident but the giant enhancement is still vague. The subplot (b) is for the laser of wavelength 1.8 μm and intensity 0.18 PW/cm^2 in which the spectral minimum is quite notable. The ATI spectra have a bell-like envelope, as shown in the H $1s$ spectra. However, because of the spectral minimum, the Xe $5p$ spectrum exhibits a double-hump structure, as is shown in the inset. For higher intensities, the giant enhancement becomes more evident, even in a linear scale, as is shown in the inset of subplot (c). The locations of the spectral minimum and of the giant enhancement are intensity independent, and these structures can be observed in a large intensity domain for various lasers. The midinfrared lasers are preferred because the required intensity is not high so that the depletion of the target can be avoided, which benefits the experimental observation. This study discloses that the momentum wave function of an atom, which is laser-field-free, modulates the envelope of both ATI and HHG spectra from the atom. Reversely, these envelope curves carry the information of atomic single-electron orbital. These spectra are fingerprints of the atomic states, from which one can deduce the laser-field free atomic wave functions.

Summary.—The spectral minimum and the giant enhancement structures exist in both the HHG spectra and the ATI spectra from driven Xe atoms. We attribute them to the inherent property of the single-electron momentum radial wave function of the Xe $5p$ subshell. The spectral minimum is caused by the nodal point in the modulus of the momentum radial wave function. The giant enhancement reflects the increase in magnitude of the momentum wave function. To observe these structures, midinfrared lasers of about 0.2 PW/cm^2 intensity are

preferred. These structures, in ATI, provide substantial evidence that they are of single-electron origin and not caused by the multielectron dynamics. Circular polarization is preferred for observing these structures in ATI spectra. These structures indicate that both the harmonic spectra and the ATI spectra are the fingerprint of the light-free Xe $5p$ state. The ATI spectra can also be used to extract information about the atomic wave function and thus provide a reference to reconstruct an atomic quantum state in tomography.

This work was supported in part by the Chinese National NSF under Grants No. 11174304 and No. 61078080 and the 973 Program of China under Grants No. 2010CB923203 and No. 2011CB808103. We thank Dr. D. Bagayoko for helpful discussions.

*jtzhang@siom.ac.cn
†dsguophd@gmail.com

[1] P. B. Corkum and F. Krausz, Nat. Phys. **3**, 381 (2007).
[2] M. Lein, N. Hay, R. Velotta, J. P. Marangos, and P. L. Knight, Phys. Rev. Lett. **88**, 183903 (2002).
[3] T. Kanai, S. Minemoto, and H. Sakai, Nature (London) **435**, 470 (2005).
[4] C. Vozzi *et al.*, Phys. Rev. Lett. **95**, 153902 (2005).
[5] P. Liu, P. Yu, Z. Zeng, H. Xiong, X. Ge, R. Li, and Z. Xu, Phys. Rev. A **78**, 015802 (2008).
[6] H. J. Worner, H. Niikura, J. B. Bertrand, P. B. Corkum, and D. M. Villeneuve, Phys. Rev. Lett. **102**, 103901 (2009).
[7] S. Haessler *et al.*, Nat. Phys. **6**, 200 (2010).
[8] B. K. McFarland, J. P. Farrell, P. H. Bucksbaum, and M. Guhr, Science **322**, 1232 (2008).
[9] O. Smirnova, Y. Mairesse, S. Patchkovskii, N. Dudovich, D. Villeneuve, P. Corkum, and M. Yu. Ivanov, Nature (London) **460**, 972 (2009).
[10] A. D. Shiner, B. E. Schmidt, C. Trallero-Herrero, H. J. Wörner, S. Patchkovskii, P. B. Corkum, J-C. Kieffer, F. Légaré, and D. M. Villeneuve, Nat. Phys. **7**, 464 (2011).
[11] D.-S. Guo, T. Aberg, and B. Crasemann, Phys. Rev. A **40**, 4997 (1989).
[12] L. Gao, X. Li, P. Fu, R. R. Freeman, and D.-S. Guo, Phys. Rev. A **61**, 063407 (2000).
[13] F. Krausz and M. Ivanov, Rev. Mod. Phys. **81**, 163 (2009).
[14] D.-S. Guo, J. Zhang, Z. Xu, X. Li, P. Fu, and R. Freeman, Phys. Rev. A **68**, 043404 (2003).
[15] H. Ye, Y. Wu, J. Zhang, and D.-S. Guo, Opt. Express **19**, 20 849 (2011).
[16] Y. Wu, H.-L. Ye, C.-Y. Shao, and J.-T. Zhang, Chin. Phys. B **21**, 024210 (2012).
[17] D.-S. Guo and G. W. F. Drake, Phys. Rev. A **45**, 6622 (1992).
[18] X. Hu, H. Wang, and D.-S. Guo, Can. J. Phys. **86**, 863 (2008).
[19] D.-S. Guo and G. W. F. Drake, J. Phys. A **25**, 3383 (1992).
[20] P. Agostini, F. Fabre, G. Mainfray, G. Petite, and N. K. Rahman, Phys. Rev. Lett. **42**, 1127 (1979).
[21] R. R. Freeman, P. H. Bucksbaum, H. Milchberg, S. Darack, D. Schumacher, and M. E. Geusic, Phys. Rev. Lett. **59**, 1092 (1987).
[22] G. D. Gillen and L. D. V. Woerkom, Phys. Rev. A **68**, 033401 (2003).
[23] M. Li, Y. Liu, H. Liu, Y. Yang, J. Yuan, X. Liu, Y. Deng, C. Wu, and Q. Gong, Phys. Rev. A **85**, 013414 (2012).
[24] Y. Wu, H.-L. Ye, J.-T. Zhang, and D.-S. Guo, Chin. Phys. B **21**, 053201 (2012).
[25] J. Zhang, W. Zhang, Z. Xu, X. Li, P. Fu, D.-S. Guo, and R. R. Freeman, J. Phys. B **35**, 4809 (2002).
[26] M. Y. Amusia, and J.-P Connerade, Rep. Prog. Phys. **63**, 41 (2000).